



UNIVERSITY OF LEEDS

This is a repository copy of *Rescue of Infectious Recombinant Hazara Nairovirus from cDNA Reveals the Nucleocapsid Protein DQVD Caspase Cleavage Motif Performs an Essential Role other than Cleavage.*

White Rose Research Online URL for this paper:
<http://eprints.whiterose.ac.uk/146558/>

Version: Accepted Version

Article:

Fuller, J orcid.org/0000-0001-8801-149X, Surtees, RA, Slack, GS et al. (3 more authors) (2019) Rescue of Infectious Recombinant Hazara Nairovirus from cDNA Reveals the Nucleocapsid Protein DQVD Caspase Cleavage Motif Performs an Essential Role other than Cleavage. *Journal of Virology*, 93 (15). e00616-19. ISSN 0022-538X

<https://doi.org/10.1128/JVI.00616-19>

© 2019 American Society for Microbiology. This is an author produced version of a paper published in *Journal of Virology*. Uploaded in accordance with the publisher's self-archiving policy.

Reuse

Items deposited in White Rose Research Online are protected by copyright, with all rights reserved unless indicated otherwise. They may be downloaded and/or printed for private study, or other acts as permitted by national copyright laws. The publisher or other rights holders may allow further reproduction and re-use of the full text version. This is indicated by the licence information on the White Rose Research Online record for the item.

Takedown

If you consider content in White Rose Research Online to be in breach of UK law, please notify us by emailing eprints@whiterose.ac.uk including the URL of the record and the reason for the withdrawal request.



eprints@whiterose.ac.uk
<https://eprints.whiterose.ac.uk/>

1 Rescue of infectious recombinant Hazara nairovirus from cDNA reveals the nucleocapsid
2 protein DQVD caspase cleavage motif performs an essential role other than cleavage.

3

4 J. Fuller¹, R. A. Surtees^{1*}, G.S. Slack², J. Mankouri¹, R. Hewson², J. N. Barr^{1§}

5

6 ¹School of Molecular and Cellular Biology, University of Leeds, Leeds, LS2 9JT, United
7 Kingdom

8 ²National Infection Service, Public Health England, Porton Down, Salisbury SP4 0JG, United
9 Kingdom

10

11 *Current address: Centre for Biological Threats and Special Pathogens, Robert Koch Institute,
12 Seestrasse 10, Berlin, 13353, Germany.

13

14 Running Title: Rescue of recombinant Hazara virus

15

16 Keywords: Hazara Virus, Rescue, Infectious Clone, Caspase, Nucleocapsid Protein

17

18 Word Count: Abstract 250; Importance 150; Main text (excluding references) - 5200

19

20 [§]To whom correspondence should be addressed Tel: 44-113-3438069; E-mail:

21 j.n.barr@leeds.ac.uk

22

23 **ABSTRACT**

24 The *Nairoviridae* family of the *Bunyvirales* order comprises tick-borne tri-segmented
25 negative strand RNA viruses, with several members associated with serious or fatal disease
26 in humans and animals. A notable member is Crimean-Congo hemorrhagic fever virus
27 (CCHFV), which is the most widely-distributed tick-borne pathogen, and associated with
28 devastating human disease with case/fatality rates averaging 30%. Hazara virus (HAZV) is
29 closely-related to CCHFV, sharing the same serogroup and many structural, biochemical and
30 cellular properties. To improve understanding of HAZV and nairovirus multiplication cycles,
31 we developed for the first time a rescue system permitting efficient recovery of infectious HAZV
32 from cDNA. This system now allows reverse genetics analysis of nairoviruses without the need
33 for high biosafety containment, as is required for CCHFV. We used this system to test the
34 importance of a DQVD caspase cleavage site exposed on the apex of the HAZV nucleocapsid
35 protein arm domain that is cleaved during HAZV infection, and for which the equivalent DEVD
36 sequence was recently shown to be important for CCHFV growth in tick but not mammalian
37 cells. Infectious HAZV bearing an un-cleavable DQVE sequence was rescued and exhibited
38 equivalent growth parameters to wild-type in both mammalian and tick cells, showing this site
39 was dispensable for virus multiplication. In contrast, substitution of the DQVD motif with the
40 similarly un-cleavable AQVA sequence could not be rescued despite repeated efforts.
41 Together, this work highlights the importance of this caspase cleavage site in the HAZV
42 lifecycle, but reveals the DQVD sequence performs a critical role aside from caspase
43 cleavage.

44

45 **IMPORTANCE**

46 Hazara virus is classified within the *Nairoviridae* family along with Crimean-Congo
47 hemorrhagic fever virus (CCHFV), which is one of the most lethal human pathogens in
48 existence, requiring the highest biosafety level (BSL) containment (BSL-4). In contrast, HAZV
49 is not associated with human disease and thus can be studied using less-restrictive BSL-2
50 protocols. Here, we report a system able to rescue Hazara virus (HAZV) from cDNAs, thus
51 permitting reverse genetic interrogation of the HAZV replication cycle. We used this system to
52 examine the role of a caspase cleavage site, DQVD, within the HAZV nucleocapsid protein
53 that is also conserved in CCHFV. By engineering mutant viruses, we showed caspase
54 cleavage at this site was not required for productive infection, and furthermore that this
55 sequence performs a critical role in the virus lifecycle aside from caspase cleavage. This
56 system will accelerate nairovirus research due to its efficiency and utility under amenable BSL-
57 2 protocols.

58

59 INTRODUCTION

60 The *Bunyavirales* order comprises over 500 RNA viruses that are the causative agents
61 of infection and disease across a broad range of hosts that encompasses insects, plants,
62 animals and humans. The bunyavirus genome comprises between 2 and 8 segments of
63 negative sense RNA, with some species utilizing an ambisense coding strategy for one or
64 more of their segments [1]. The recent use of metagenomic techniques [2], [3], [4] has led to
65 the discovery of many new diverse bunyaviruses, particularly from within arthropod hosts, and
66 so bunyavirus classification is in a state of flux. Currently, the order is divided into twelve
67 families [1], and viruses associated with human infections are classified within five of these,
68 namely the *Arenaviridae*, *Hantaviridae*, *Nairoviridae*, *Peribunyaviridae* and *Phenuiviridae*
69 families. The *Nairoviridae* family comprises tick-borne tri-segmented RNA viruses, with
70 several members associated with serious and fatal disease in both humans and animals.
71 Nairobi sheep disease virus, after which the family was named, causes acute gastroenteritis
72 in susceptible populations of sheep and goats, with an associated mortality rate of 90%,
73 resulting in significant economic impact [5]. Crimean-Congo hemorrhagic fever virus (CCHFV)
74 is the most widely distributed tick-borne pathogen on earth [6], and is associated with a
75 devastating human disease known as Crimean-Congo hemorrhagic fever (CCHF) with
76 case/fatality rates averaging 30%, but rising as high as 80% in specific outbreaks [7], [8].
77 CCHF most commonly results from the bite of a CCHFV-infected tick of the *Hyalomma*
78 species, which is widespread within Africa, South-East Europe and Asia, and concerns are
79 growing over the widening habitat of permissive tick vectors in the face of global warming [9]–
80 [12]. Due to the associated risks, CCHFV is one of a select group of pathogens classified
81 within hazard group 4, requiring the highest level of biological containment for its propagation
82 (biosafety level 4; BSL-4), which has restricted research activity and hindered progress in
83 elucidating the molecular and cellular biology of CCHFV, as well as nairoviruses in general.

84 Hazara virus (HAZV) is a nairovirus that is closely related to CCHFV, such that it is
85 included within the same serogroup [1], however, it is non-pathogenic in humans. As a

86 consequence, HAZV can be studied in relatively accessible BSL-2 facilities, which permits
87 more rapid and cost-effective research.

88 The genomes of HAZV and CCHFV are tri-segmented, comprising small (S), medium
89 (M) and large (L) segments. The S segment of both viruses encodes the nucleoprotein (N),
90 which encapsidates the RNA segments through its RNA binding ability. In addition, the
91 CCHFV S segment is thought to express an additional non-structural protein (NSs) using an
92 ambi-sense transcription strategy, with a role in apoptotic activation [13]. The M segment
93 encodes the glycoprotein precursor GPC that is subsequently cleaved into the structural
94 glycoproteins Gn and Gc, and additional non-structural glycoproteins, whereas the L segment
95 encodes the relatively large RNA-dependent RNA polymerase (RdRp) [14], which is involved
96 in replication and transcription of viral RNA, but also encodes an N terminal ovarian tumour
97 (OTU) domain with roles in mitigating host cell innate immunity [15].

98 We and others recently solved the crystal structure of the N protein of both HAZV and
99 CCHFV, which revealed the location of a conserved caspase-3 cleavage (C3C) site on the
100 exposed apex of the extended arm domain suggestive of an important role at some stage of
101 the nairovirus multiplication cycle [16]–[19]. One possibility was that the C3C site acted as a
102 caspase-3 decoy, diverting caspase-3 away from its native cellular substrates and thus
103 preventing or prolonging apoptosis activation, as has recently been found for the related Junin
104 arenavirus (JUNV) [20]. In support of this, both CCHFV and HAZV-N proteins are extensively
105 cleaved at their C3C sites in mammalian cells, with apoptosis induced relatively late in infection
106 [21],[22]. However, during infection by both HAZV and CCHFV in tick cell lines, the C3C site
107 is subjected to little or no cleavage, revealing a fundamental difference in the tick and
108 mammalian cellular response to nairovirus infection [23],[22]. Recently, a system capable of
109 rescuing infectious CCHFV from cDNA was used to show that the conserved C3C site on the
110 arm apex was dispensable for infection in mammalian cells, but strikingly mutation of this motif
111 resulted in a significant drop in replication ability during infection of cells of tick origin [23].
112 Taken together, these findings revealed a critical role for the C3C site for CCHFV growth in
113 ticks, although whether the C3C site in HAZV was required remained unknown.

114 Here, we developed a system for the rescue of infectious HAZV to authentically-test
115 the importance of caspase cleavage of HAZV-N during infection. By generating a panel of
116 mutant viruses in which the arm domain DQVD was rendered un-cleavable, we showed while
117 this sequence was critical for virus viability, it was not to allow caspase cleavage. Instead, our
118 results show that the DQVD site performs a critical role in the virus life cycle aside from acting
119 as a caspase substrate. To the best of our knowledge, this work represents the first recovery
120 of recombinant HAZV (rHAZV) and also the first nairovirus rescue system that permits virus
121 rescue in BSL-2 facilities, thus facilitating rapid future gains in the understanding of this
122 important group of viruses.

123

124

125 RESULTS

126 **Characterization of the DQVD caspase cleavage site in HAZV-N.** In previous work,
127 we identified a number of HAZV-N specific cleavage products during low-MOI infection of
128 mammalian cells [22]. To further characterise these bands, we repeated HAZV infection of
129 human-origin SW13 cells at a higher MOI of 1.0 to increase presence of these cleaved forms
130 of HAZV-N thereby facilitating detection via western blotting. HAZV-N antisera detected
131 prominent N-specific cleavage products with apparent molecular masses of approximately 30
132 and 22 kDa, and exhibiting a temporal expression pattern, being absent during initial stages
133 of infection, and most abundant at later time points (Fig 1A). Previous work by ourselves and
134 others [16], [19] established that the generation of 30 and 22 kDa products resulted from
135 caspase-3 cleavage of HAZV-N at a consensus DQVD motif (Fig 1B) located at the apex of
136 the HAZV-N arm domain (Fig 1C). The HAZV-N arm domain also possesses the sequence
137 ENKD, which partially-conforms to the caspase-3 cleavage consensus sequence, and is
138 immediately upstream of the DQVD such that these sites overlap forming the sequence
139 ENKDQVD.

140

141 **Recovery of recombinant HAZV.** In order to investigate the role of the ENKD/DQVD
142 caspase cleavage motifs in the authentic context of HAZV infection, we generated a cDNA-
143 based system to allow rescue of infectious HAZV. This system comprised three cDNA
144 plasmids that were designed to transcribe the anti-genomic cRNA strands of the HAZV S, M
145 and L segments under the control of the bacteriophage T7 RNA polymerase promoter, an
146 approach that has been used by others to rescue bunyaviruses of the *Arenaviridae*,
147 *Peribunyaviridae* and *Phenuiviridae* families, as well as CCHFV from the *Nairoviridae* family
148 [24]–[27]. The three corresponding plasmids pMK-RQ-S, pMK-RQ-M and pMK-RQ-L were co-
149 transfected into BSR-T7 cells expressing T7 RNA polymerase, along with plasmid pCAG-
150 T7pol, which allows increased expression of the T7 RNA polymerase, and in our hands further
151 increases the efficiency of virus recovery (Fig 2A). Additional transfections in which HAZV L

152 segment expression plasmid pMK-RQ-L was omitted were also performed, to act as rescue
153 controls incapable of generating infectious virus.

154 In cells transfected with all four plasmids ('complete transfection'), HAZV-N protein
155 was abundantly detected by western blotting in the primary transfected cultures at 120 hours
156 post transfection (p.Tr) (Fig 2B; p.Tr , lane 1) suggestive of HAZV rescue. As confirmation,
157 supernatants of primary transfected cultures at 72-, 96- and 120-hours p.Tr were harvested
158 and used to infect further SW13 cells in order to amplify any rescued viruses. At 48-hours post
159 infection (p.Inf) SW13 cell lysates were harvested and tested for presence of HAZV-N by
160 western blot analysis, which revealed abundant N production in 96- and 120-hours p.Inf
161 samples, confirming virus amplification had occurred (Fig 2B; p.Inf, lanes 2-4). Rescue of WT
162 rHAZV was achieved in all attempts using this optimized protocol, indicating the system was
163 robust and efficient.

164 In contrast, HAZV-N protein was not detected in control transfected cells that received
165 no pMK-RQ-L ('control transfection') in primary transfected cells (Fig 2B; p.Tr , lane 5), and
166 correspondingly, no N was detected in cell lysates harvested at any time points in the p.Inf
167 wells (Fig 2B; p.Inf, lanes 6-8).

168 To examine the efficiency of HAZV rescue, supernatant samples taken from primary
169 transfected BSR-T7 cells at 72-, 96- and 120-hours p.Tr time points were used to set up plaque
170 assays in SW13 cells. Analysis of the resulting plaques formed showed increasing titres of
171 rHAZV in the p.Tr supernatant increasing through 72-, 96- and 120-hours p.Tr time points (Fig
172 2C), with titres of rescued virus reaching over 1.2×10^5 pfu/ml in the 120-hours p.Tr
173 supernatants.

174

175 **Comparison of HAZV and rHAZV growth kinetics.** Although the rescued virus was
176 generated from a cDNA source corresponding precisely to HAZV strain JC280, we wanted to
177 verify that rHAZV displayed equivalent growth properties to the parental JC280 isolate, which
178 may have acquired cell culture adaptations through multiple rounds of propagation. To achieve
179 this, we compared multi-step growth kinetics of rHAZV alongside the parental virus isolate and

180 mock-infected controls. Following infection at an MOI of 0.001, supernatant samples from
181 each infection scenario were harvested every 24 hours for up to 96 hours p.Inf, and used to
182 titre infectious virus by plaque assay (Fig 3A). Similar titres for HAZV and rHAZV were
183 observed at all time points, indicating infectious rHAZV displayed equivalent growth kinetics
184 to the parental virus. Plaque morphology of rHAZV also resembled that of the parental virus
185 (Fig 3B), providing further evidence that recombinant and parental viruses possessed
186 indistinguishable growth properties.

187

188 **Confirmation of HAZV rescue from a cDNA source by incorporation of a silent**
189 **mutation.** To confirm the recombinant source of rHAZV as cDNA, a single nucleotide change
190 of G723T in the N protein open reading frame (ORF) was engineered into pMK-RQ-S to create
191 pMK-RQ-S(G723T). This change was silent at the amino acid level, but generated a *Hind* III
192 recognition site in the corresponding cDNA sequence (Fig 4A). Plasmid pMK-RQ-S(G723T)
193 replaced the corresponding WT pMK-RQ-S plasmid in a HAZV recovery experiment alongside
194 WT rescue plasmids pMK-RQ-M, pMK-RQ-L, and pCAG-T7pol, described above, and western
195 blotting of post-infection lysates revealed the abundant presence of HAZV-N indicating
196 successful mutant virus recovery (Fig 4B). To verify incorporation of the G723T change, RNA
197 extracted from rHAZV and rHAZV(G723T) infected SW13 cell supernatants was used as a
198 template for RT-PCR amplification, using primers designed to yield an 802 nucleotide-long
199 cDNA fragment encompassing the *Hind* III site. While the WT cDNA fragment was un-cleaved
200 by *Hind* III, the corresponding fragment from rHAZV(G723T) was cleaved to generate two
201 products with lengths of approximately 300 and 500 bp (Fig 4C and 4D), corresponding to the
202 fragments expected following *Hind* III digestion. To confirm that the amplified PCR fragment
203 was templated from a cDNA that originated from an RNA source rather than plasmid carried
204 over from the transfections, we also performed control PCR amplifications without prior RT
205 treatment, and these failed to yield a DNA fragment (Fig 4D). Successful rescue of this rHAZV
206 variant was also confirmed by sequencing of the RT-PCR fragment bearing the introduced

207 *Hind* III recognition site. Taken together, these findings confirm the utility of the rescue system
208 to efficiently generate both WT and mutant rHAZV variants.

209

210 **Rescue of infectious HAZV variants with alterations to caspase cleavage sites**

211 **on the N protein arm apex.** Previous work from ourselves and others has identified caspase-
212 3 cleavage motifs on both the CCHFV N (DEVD) and the HAZV-N (DQVD) proteins at the
213 apex of their respective arm domains [16], [17], [19] and mapping these sites onto the
214 corresponding crystal structures show these are in precisely superimposable positions (Fig
215 5A). Both sites also are preceded by sequences that partially-conform to caspase cleavage
216 consensus sequences suggesting that their cleavage is possible, but nevertheless unlikely.
217 These sequences are KHKD in CCHFV and ENKD in HAZV, and both sites overlap the
218 established DEVD/DQVD cleavage sites at a critical aspartic acid residue (D) (Fig 5A). Both
219 DEVD and DQVD sites are known to be cleaved during infection of mammalian cells by
220 CCHFV and HAZV, respectively [22], [21], and a mutant CCHFV with the DEVD site changed
221 to the non-cleavable AEVA site was shown to be severely growth-attenuated in tick cells, but
222 phenotypically-silent when growth in cells of mammalian origin [23].

223 To investigate the importance of the DQVD and overlapping ENKD motifs in the
224 context of HAZV infection (Fig 1A and 5A), we created mutant plasmids designed to express
225 HAZV S segments in which the ENKD and DQVD motifs within the N ORF were individually
226 perturbed by mutation. The aspartic acid (D) residues at position 1 within these motifs
227 (underlined) are known to be critical for caspase recognition and cleavage [28], and so in both
228 cases, this residue was changed to glutamic acid (E) to generate the non-cleavable
229 sequences ENKE and DQVE. An additional double mutant plasmid with the sequence AQVA
230 was also generated, concurrently rendering both ENKD and DQVD motifs as un-cleavable,
231 and allowing direct comparison with the AEVA mutant generated for CCHFV, described above
232 [23].

233 As with the rHAZV recoveries described above, the plasmid expressing the WT HAZV
234 S segment pMK-RQ-S, or its mutant derivatives (named correspondingly DQVE, ENKE or

235 AQVA) were transfected into BSR-T7 cells along with pMK-RQ-M, pMK-RQ-L, and pCAG-
236 T7pol, and at 72-, 96- and 120-hours p.Tr supernatants were collected and used to re-infect
237 fresh SW13 monolayers for 48 hours. At this time point, lysates were collected and examined
238 for HAZV-N expression via western blotting with anti-HAZV-N antisera (Fig 5A) with HAZV-N
239 detection in virus rescue wells indicating successful recovery of both recombinant WT and
240 mutant viruses. Successful rescue was achieved for HAZV-N mutants rHAZV-DQVE and
241 rHAZV-ENKE, with rescue confirmed by sequencing of an RT-PCR fragment bearing the
242 altered cleavage sites (data not shown) amplified from viral RNA harvested from p.Inf
243 supernatants. In contrast, double mutant rHAZV-AQVA could not be rescued, as evidenced
244 by three failed rescue attempts alongside consistent successful rescue of WT rHAZV.

245 The growth kinetics of rescued rHAZV-ENKE and rHAZV-DQVE were examined
246 alongside WT rHAZV via plaque assay over a 4-day time course (Fig 5B), and morphology of
247 resulting plaques was assessed (Fig 5C). Viral titres at all time points tested showed no
248 significant differences between WT rHAZV and the rHAZV-ENKE or rHAZV-DQVE mutants
249 (Fig 5D) and taken together these results show that abrogating caspase cleavage at either of
250 these sites has no detectable effect on virus fitness.

251

252 **The HAZV-N DQVD caspase cleavage motif is required for rescue of infectious**
253 **virus, but for reasons other than caspase cleavage.** The results of the previous section
254 showed HAZV mutants bearing un-cleavable DQVE and ENKE sequences in N could be
255 rescued, whereas an AQVA mutant could not. As expected, abrogation of cleavage at the
256 DQVD site coincided with loss of the customary 30 kDa HAZV-N cleavage product, as
257 measured by western blot analysis (Fig 5E). Interestingly, this band was replaced by a band
258 of increased apparent mass, corresponding to approximately 32 kDa. This 32 kDa HAZV-N
259 fragment is too large to correspond to alternative cleavage at the adjacent and overlapping
260 ENKD, so our results show that during infection with the rHAZV-DQVE mutant, N cleavage at
261 neither the overlapping ENKD site, nor the altered DQVE site, occurs. The fact that infection
262 with the DQVE mutant does not result in generation of a 30 kDa fragment also shows the

263 ENKD site is not a substrate for caspase cleavage even when the DQVD site can no longer
264 be cleaved, consistent with its only partial similarity to the caspase cleavage consensus.
265 Taken together, these results show that HAZV-N lacking a functional caspase cleavage site
266 at the arm apex can be rescued as infectious virus, and thus a caspase cleavable site at the
267 arm apex is not a prerequisite for HAZV viability.

268 Thus, our results show that individually, the DQVD and ENKD motifs are dispensable
269 for the HAZV life-cycle in cultured mammalian cells. However, our observation that the double
270 mutant AQVA could not be rescued despite repeated attempts suggests that simultaneous
271 alteration of both sites critically-prevents virus multiplication at some stage of the life cycle. As
272 we show above that cleavage within the arm domain is not required for virus viability, we
273 suggest the fatal deficiency of the AQVA mutant relates to a function other than caspase
274 cleavability.

275 This observation is interesting in comparison to the previous findings for CCHFV that
276 the corresponding AEVA mutant, which also acts as a double mutant knocking out both KHKD
277 and DEVD sites, could be rescued as infectious virus, and furthermore replicated to wild-type
278 (WT) titres in mammalian cells [23]. Taken together, these findings suggest that sequences
279 within the arm apex of CCHFV and HAZV perform different roles, with those of HAZV being
280 highly sensitive to change, with those of CCHFV being more tolerant.

281

282 **The DQVD caspase-3 cleavage motif is also dispensable for HAZV replication in**
283 **cells of tick origin.** As described above, previous work by others has shown that a CCHFV
284 variant with an un-cleavable AEVA substitution at the N protein arm apex DEVD site replicates
285 to WT titres in SW13 cells, but cannot replicate in tick cells, suggesting a critical role for this
286 motif in the CCHFV life cycle [23]. Having shown that mutations at caspase cleavage sites
287 ENKD or DQVD at this location on HAZV-N pose no significant reduction in growth in
288 mammalian cells (Fig 5C), we next wanted to examine the role of these motifs for replication
289 in tick cells.

290 To achieve this aim, we examined the ability of the rHAZV-DQVE and rHAZV-ENKE
291 variants to multiply in CTVM/HAE9 tick cells, as determined by their ability to express
292 abundant HAZV-N after 48 hours (Fig 6A). Infection with rHAZV carrying individual DQVE and
293 ENKE substitutions resulted in the synthesis of equivalent quantities of N as WT rHAZV, as
294 measured by western blot analysis with HAZV-N antisera, categorically showing that the
295 corresponding DQVD and ENKD motifs are non-essential for rHAZV replication in cells of tick
296 origin, when individually altered. The equivalent abundance of N proteins expressed by these
297 viruses compared to WT also suggested these viruses were not growth attenuated in these
298 cells.

299 A more direct comparison between the role of the arm apex cleavage sites of CCHFV
300 and HAZV would be achieved using equivalent substituting sequences; AEVA for CCHFV and
301 AQVA for HAZV. However, this comparison was not possible, as the AQVA mutant for HAZV
302 could not be rescued, despite repeated efforts. Nevertheless, these results show the ability of
303 the DQVE virus to replicate in tick cells does not require a cleavable caspase site on the apex
304 of the N arm domain.

305

306 DISCUSSION

307 Here, we report a rescue system allowing the production of infectious HAZV from
308 cDNA that can be utilized in widespread and amenable BSL-2 facilities, and which represents
309 an important advance in the study of nairovirus molecular and cellular biology. Previously, a
310 rescue system for the highly-pathogenic CCHFV was established, permitting insight into the
311 role of multiple nairovirus specific features such as the OTU domain within the L protein ORF,
312 as well as characterization of the processing pathway of GPC, expressed from the M segment
313 ORF [15], [27]. However, due to the extreme pathogenicity of CCHFV, utilization of this rescue
314 system has been restricted to a small number of laboratories that can comply with the highest
315 BSL-4 containment protocols. The development of a HAZV rescue system that can be utilized
316 using less-restrictive BSL-2 protocols will greatly facilitate and accelerate future nairovirus
317 research. A HAZV mini-genome system has also been reported recently [29], which allowed
318 the delineation and characterization of the viral mRNA transcription promoters, and while utility
319 of this system is restricted to analysis of *cis*-acting signals involved in RNA synthesis, it will
320 also allow a rapid accumulation of information regarding nairovirus multiplication.

321 The HAZV rescue system we describe here was capable of generating a titre of WT
322 HAZV of over 1.2×10^5 pfu/ml in primary transfection supernatants. Correspondingly, rescue
323 of WT rHAZV was successful in every attempt, and allowed rescue of each of the mutants
324 described in this manuscript with minimal experimental replicates. Taken together these
325 findings suggest the HAZV rescue system is highly efficient, a property that will facilitate the
326 rescue of mutant viruses that possess other attenuating lesions.

327 The N proteins of both HAZV and CCHFV possess caspase-3 cleavage motifs with the
328 sequences DQVD and DEVD, respectively [16], [30], prominently located at equivalent
329 positions on the apex of their arm domains, suggesting their conservation is driven by
330 functional importance. In line with this suggestion, previous work has shown both HAZV and
331 CCHFV N proteins are cleaved *in vitro* at these motifs by purified active caspase-3 [16], [17],
332 [19], as well as by caspase-3 in cultured human cells [22].

333

334 To test the importance of cleavage within the HAZV-N arm domain during HAZV
335 infection, we generated mutant viruses for which the overlapping ENKD and DQVD consensus
336 cleavage sites were individually disrupted with glutamic acid substitutions at position 1
337 (underlined) to render them un-cleavable. The fact that both the resulting viruses rHAZV-
338 ENKE and rHAZV-DQVE were viable and replicated with growth kinetics that were
339 indistinguishable from WT rHAZV is a critical observation. Because the DQVE mutant is
340 cleaved at neither this DQVE site, nor the adjacent ENKD site (Fig 5C), these findings show
341 cleavage within the arm apex is not a requirement for virus viability.

342 Our failure to rescue the rHAZV-AQVA mutant despite repeated efforts suggests it is
343 deficient in a critical function. We show that caspase cleavage within the arm apex is not a
344 requirement for virus viability, and indeed viruses that cannot be cleaved at this location show
345 equivalent fitness to WT HAZV. Thus, the lack of rescue of rHAZV-AQVD cannot be due to
346 loss of cleavability of the arm apex. This finding is intriguing in light of recent work with CCHFV
347 for which the equivalent AEVA mutant was found to be phenotypically-silent in mammalian
348 cells but significantly reduced in fitness for replication in tick cells. These findings suggest the
349 requirements for HAZV and CCHFV are different, and the molecular basis for these
350 differences likely lie in the subtle differences of arm domain sequences (Figure 5A). Our
351 results here show the DQVD site is important for rescue, but not for caspase cleavage and
352 this provides a starting point for studies to elucidate the critical role of this DQVD motif. So
353 what might this possible role be? One possibility is in N-N multimerization. Previous work has
354 shown the crystallographic N-N interface between adjacent monomers involves the formation
355 of a hydrophobic pocket comprising six residues from the arm domain of one monomer that
356 interacts with a single proline residue located on the base of the globular domain of the adjacent
357 monomer [16]. Interestingly, neither aspartate (D) residues within the DQVD motif that are
358 altered in either DQVE or AQVA mutants are involved in this interaction, which would thus
359 appear to rule out N-N interactions as its critical role. However, we cannot rule out the
360 possibility that the HAZV N-N interaction that occurs in the assembly of an authentic nairovirus
361 ribonucleoprotein (RNP) is different to that revealed in the HAZV N crystal structure, and that

362 these critical aspartate residues do indeed play important roles in RNP formation. This matter
363 will be resolved by solving the structure of nairovirus RNPs in their native state. An alternative
364 possibility is that the DQVD site is involved in an interaction with a host factor, and the
365 availability of such a component may also explain the differential outcome of infection with
366 CCHFV in mammalian and tick cells.

367 Previous work by ourselves and others has suggested that caspase cleavage of the
368 nairovirus N protein may act as a caspase decoy, as has been shown for JUNV. Our results
369 presented here showing the essential role of the HAZV DQVD motif is essential for a role other
370 than cleavage does not rule this out. In fact, the finding that the rHAZV-DQVE mutant no
371 longer generates the customary 30 kDa band, but instead is cleaved to yield a 32 kDa product
372 shows that alternative cleavage sites exist that are amenable to cleavage once the dominant
373 sites are removed. Deciphering the caspase cleavage profile of nairovirus N proteins is a
374 complex task, as for HAZV there are a total of 28 aspartate residues that could potentially be
375 cleaved, however we are struck by the high accessibility of the HAZV N protein to caspase
376 digestion. Further work on this and other projects are currently underway, using the rescue
377 system described here, and we hope that its use will accelerate further understanding of
378 nairovirus molecular and cellular biology.

379

380 **MATERIALS AND METHODS**

381 **Cells and viruses.** BSR-T7 cells (derived from baby hamster kidney, containing a T7
382 polymerase expression gene) were maintained in Dulbecco's modified Eagle medium (DMEM)
383 (Sigma Aldrich) containing 2.5 % foetal bovine serum (FBS) (Invitrogen). SW13 cells (derived
384 from human adrenal cortex) were maintained in DMEM containing 10 % FBS. All cell culture
385 media were supplemented with 100 U/ml penicillin and 100 µg/ml streptomycin and grown at
386 37 °C in a 5 % CO₂ atmosphere. Tick-derived HAE/CTVM9 (*Hyalomma anatolicum*) cells [31]
387 were maintained in L15 / MEM containing 20 % FBS, 10 % tryptose phosphate broth, 2 mM
388 L-glutamine, 100 U/ml penicillin and 100 µg/ml streptomycin at 30 °C.

389

390 **Plasmids.** Full-length cDNAs representing the S, M and L segments were synthesized
391 (Genewiz) using the HAZV strain JC280 (Genebank accession numbers: M86624.1,
392 NC_038710 and DQ076419.1, respectively) as reference and incorporated into the pMK-RQ
393 plasmid, resulting in the generation of pMK-RQ-S, pMK-RQ-M and pMK-RQ-L, able to express
394 S, M and L segment-specific RNAs, respectively. Viral gene segments were flanked by the
395 bacteriophage T7 polymerase promoter, and hepatitis delta virus ribozyme to ensure correct
396 formation of 3' and 5' terminal sequences, with the cDNAs orientated such that primary T7
397 polymerase transcripts were of positive sense. pCAG-T7pol was a gift from Ian Wickersham
398 (Addgene plasmid #59926). Generation of mutant plasmids was achieved using the Q5 Site
399 Directed Mutagenesis (SDM) kit (New England Biolabs) according to the manufacturer's
400 instructions, with all mutant plasmid sequences confirmed via sequencing (Genewiz)

401

402 **Virus rescue.** Six-well plates were seeded with 2×10^5 BSR-T7 cells/well 1 day prior to
403 transfection in 2 ml DMEM supplemented with 2.5 % FBS. 16-24 hours later, cells were
404 transfected with 1.2 μ g of pMK-RQ-S, pMK-RQ-M, pMK-RQ-L and 0.6 μ g pCAG-T7pol,
405 combined with 2.5 μ l Mirus TransIT-LT1 transfection reagent (Mirus Bio) per μ g of DNA in 200
406 μ l OPTI-MEM (Life Technologies). For mutant recovery, the WT plasmid was replaced with
407 the corresponding mutant plasmid. A control sample was set up alongside each experiment
408 in which transfection of pMK-RQ-L was omitted. Cell supernatants were collected 72-, 96- and
409 120-hours post transfection and 300 μ l supernatant was passaged in a 6-well plate of SW13
410 cells grown in DMEM supplemented with 10 % FBS for 48 hours. 100 μ l supernatant was also
411 used to titre virus following transfection using a standard plaque assay protocol.

412

413 **Virus infections.** SW13 monolayers were infected with HAZV at the specified
414 multiplicity of infection (MOI) in serum-free DMEM (SFM) at 37 °C. After 1 hour, the inoculum
415 was removed and cells washed in phosphate buffered saline (PBS), fresh DMEM containing

416 2.5 % FBS, 100 U/ml penicillin and 100 µg/ml streptomycin was then applied for the duration
417 of the infection. Infections of HAE/CTVM9 cells of tick origin were carried out at an MOI of
418 0.01 in a similar manner to mammalian cell infections, but with an incubation temperature of
419 30 °C.

420

421 **Inhibition of caspases.** SW13 monolayers were pre-treated with 20 µM Z-FA-FMK
422 for 45 minutes in SFM at 37 °C prior to infection with HAZV at an MOI of 0.1. Following
423 infection, virus and inhibitor were removed, cells were washed three times in PBS and 2.5%
424 FBS DMEM was reapplied containing 20 µM Z-FA-FMK. At 24-, 32- and 48-hours timepoints
425 total cell lysates were harvested and prepared for western blot.

426

427 **Cell viability assays.** SW13 monolayers were pre-treated with a range of Z-FA-FMK
428 concentrations for 1 hour 45 minutes in SFM, matching the duration of the pre-treatment and
429 infection stage. At this point, media was changed to 2.5% FBS DMEM containing the same
430 concentration of drug, again matching the infection procedure. Following a 48-hours infection
431 period, cell viability was assessed using the CellTiter 96® AQueous One Solution Cell
432 Proliferation Assay (Promega) according to the manufacturer's instructions.

433

434 **Western blotting.** For preparation of cell lysates, monolayers were washed in ice cold
435 PBS followed by incubation in ice cold RIPA buffer (150 mM sodium chloride, 1.0% NP-40
436 alternative, 0.1% SDS, 50 mM Tris, pH 8.0) and agitated for 120 seconds. Cells were then
437 harvested via cell scraping and transferred to pre-chilled Eppendorf tubes, after which lysates
438 were centrifuged at 20,000 x g for 15 minutes to pellet insoluble material. SDS-gel loading
439 buffer containing DTT was added to the supernatant prior to storage at -20°C. Proteins were
440 separated on 12 % SDS polyacrylamide gels by electrophoresis and transferred to
441 fluorescence compatible PVDF (FL-PVDF) membranes. Sheep anti-HAZV-N antiserum
442 generated as previously described [32] was used to detect HAZV-N, and was subsequently

443 visualised using fluorescently labelled anti-sheep secondary antibodies. Membranes were
444 visualised on the LiCor Odyssey Sa Infrared imaging system.

445

446 **Virus titration.** Determination of virus titre for construction of growth curves was
447 achieved through plaque assay. Briefly, SW13 cells were seeded (2×10^6) into 75 cm² flasks
448 24 hours prior to infection with HAZV, rHAZV or mutant rHAZV at an MOI of 0.001.
449 Supernatant was collected at time points of 24-, 48-, 72-, 96- and 120-hours post infection,
450 and serially-diluted to infect fresh monolayers of SW13 cells in a 6-well plate. Following
451 infection, media containing virus was removed and replaced with 1:1 2.5 % FBS DMEM and
452 1.6 % methylcellulose and returned to incubate for a further 6 days prior to fixing and staining
453 with crystal violet. Plaques were then counted and virus titre determined.

454

455 **Extraction of viral RNA.** Viral RNA was first extracted from cell-free supernatant using
456 the Qlamp Viral RNA kit (Qiagen) and treated with DNase to remove any contaminating DNA
457 before a cDNA copy was generated using ProtoScript II Reverse Transcriptase (New England
458 Biolabs) according to manufacturer's instructions. PCR amplification of an ≈ 800 bp fragment
459 using primers specific to the HAZV S segment was achieved using the Q5 High Fidelity
460 Polymerase (New England Biolabs). Restriction digest analysis was performed by incubating
461 *Hind* III (New England Biolabs) with 500 ng PCR product at 37 °C for 1 hour prior to resolving
462 DNA bands on a 1 % agarose gel containing 0.01 % SYBR Safe (ThermoFisher).

463

464 **ACKNOWLEDGEMENTS**

465 The authors would like to thank Dr Bell-Sakyi and the Tick Cell Biobank, University of
466 Liverpool, Liverpool, UK for kindly providing HAE/CTVM9 cells.

467

468 **AUTHOR CONTRIBUTIONS**

469 Author contributions are as follows: JF, RAS, GS, RH, JM and JNB conceptualized the study;
470 JF, RAS, GS performed the experimental investigation; JF and JNB wrote the original draft
471 manuscript; RAS and GS reviewed and edited the manuscript; JM, RH and JNB supervised
472 the core team; JNB provided management and coordination of the research activities and
473 acquired the financial support for the project.

474

475 **CONFLICTS OF INTEREST**

476 The authors declare that there are no conflicts of interest.

477

478 **FUNDING**

479 This work was funded by a Public Health England (PHE) PhD studentship (to J. Fuller)

480

481 **References**

- 482 [1] ICTV, "Virus Taxonomy," 2018. [Online]. Available:
483 <https://talk.ictvonline.org/taxonomy/>. [Accessed: 14-Jan-2018].
- 484 [2] N. Makhsous, R. C. Shean, D. Droppers, J. Guan, K. R. Jerome, and A. L. Greninger,
485 "Genome Sequences of Three Novel Bunyaviruses, Two Novel Rhabdoviruses, and
486 One Novel Nyamivirus from Washington State Moths," *Genome Announc.*, vol. 5, no.
487 7, pp. e01668-16, Feb. 2017.
- 488 [3] J. Bouquet, M. Melgar, A. Swei, E. Delwart, R. S. Lane, and C. Y. Chiu, "Metagenomic-
489 based Surveillance of Pacific Coast tick *Dermacentor occidentalis* Identifies Two Novel
490 Bunyaviruses and an Emerging Human Rickettsial Pathogen," *Sci. Rep.*, vol. 7, no. 1,
491 p. 12234, 2017.
- 492 [4] J. A. Chandler, R. M. Liu, and S. N. Bennett, "RNA Shotgun Metagenomic Sequencing
493 of Northern California (USA) Mosquitoes Uncovers Viruses, Bacteria, and Fungi," *Front.*
494 *Microbiol.*, vol. 6, p. 185, 2015.
- 495 [5] F. G. Davies, "Nairobi sheep disease," *Parassitologia*, vol. 39, no. 2, pp. 95–98, 1997.
- 496 [6] J. P. Messina, D. M. Pigott, N. Golding, K. A. Duda, J. S. Brownstein, D. J. Weiss, H.
497 Gibson, T. P. Robinson, M. Gilbert, G. R. William Wint, P. A. Nuttall, P. W. Gething, M.
498 F. Myers, D. B. George, and S. I. Hay, "The global distribution of Crimean-Congo
499 hemorrhagic fever," *Trans. R. Soc. Trop. Med. Hyg.*, vol. 109, no. 8, pp. 503–513, 2015.
- 500 [7] O. Ergonul and C. A. Whitehouse, *Crimean-Congo hemorrhagic fever: A global*
501 *perspective*. 2007.
- 502 [8] T. F. Schwarz, H. Nsanze, and A. M. Ameen, "Clinical features of Crimean-Congo
503 haemorrhagic fever in the United Arab Emirates," *Infection*, 1997.
- 504 [9] G. Grard, J. F. Drexler, J. Fair, J. J. Muyembe, N. D. Wolfe, C. Drosten, and E. M.
505 Leroy, "Re-Emergence of Crimean-Congo hemorrhagic fever virus in central Africa,"
506 *PLoS Negl. Trop. Dis.*, 2011.
- 507 [10] A. M. Palomar, A. Portillo, S. Santibáñez, L. García-Álvarez, A. Muñoz-Sanz, F. J.
508 Márquez, L. Romero, J. M. Eiros, and J. A. Oteo, "Molecular (ticks) and serological

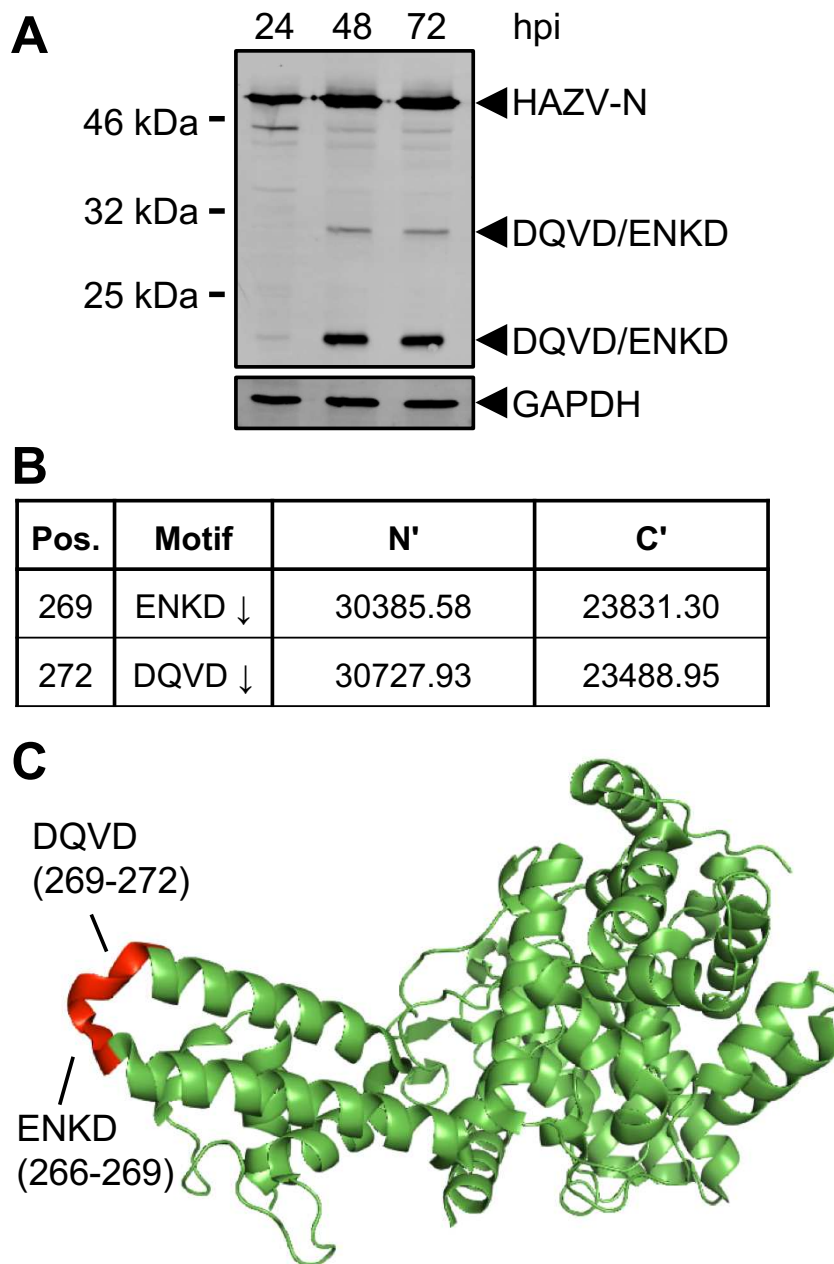
- 509 (humans) study of Crimean-Congo hemorrhagic fever virus in the Iberian Peninsula,
510 2013–2015,” *Enfermedades Infecc. y Microbiol. Clin. (English ed.)*, vol. 35, no. 6, pp.
511 344–347, 2017.
- 512 [11] S. K. Al-Tikriti, F. Al-Ani, F. J. Jurji, H. Tantawi, M. Al-Moslih, N. Al-Janabi, M. I.
513 Mahmud, A. Al-Bana, H. Habib, H. Al-Munthri, S. Al-Janabi, K. AL-Jawahry, M. Yonan,
514 F. Hassan, and D. I. Simpson, “Congo/Crimean haemorrhagic fever in Iraq,” *Bull. World*
515 *Health Organ.*, vol. 59, no. 1, pp. 85–90, 1981.
- 516 [12] A. Papa, I. Christova, E. Papadimitriou, and A. Antoniadis, “Crimean-Congo
517 hemorrhagic fever in Bulgaria,” *Emerg. Infect. Dis.*, vol. 10, no. 8, pp. 1465–1467, 2004.
- 518 [13] B. Barnwal, H. Karlberg, A. Mirazimi, and Y.-J. Tan, “The Non-structural Protein of
519 Crimean-Congo Hemorrhagic Fever Virus Disrupts the Mitochondrial Membrane
520 Potential and Induces Apoptosis,” *J. Biol. Chem.*, vol. 291, no. 2, pp. 582–592, 2016.
- 521 [14] M. Zivcec, F. E. M. Scholte, C. F. Spiropoulou, J. R. Spengler, and É. Bergeron,
522 “Molecular insights into Crimean-Congo hemorrhagic fever virus,” *Viruses*. p. 106,
523 2016.
- 524 [15] F. E. M. Scholte, M. Zivcec, J. V. Dzimianski, M. K. Deaton, J. R. Spengler, S. R. Welch,
525 S. T. Nichol, S. D. Pegan, C. F. Spiropoulou, and É. Bergeron, “Crimean-Congo
526 Hemorrhagic Fever Virus Suppresses Innate Immune Responses via a Ubiquitin and
527 ISG15 Specific Protease,” *Cell Rep.*, vol. 20, no. 10, pp. 2396–2407, 2017.
- 528 [16] R. Surtees, A. Ariza, E. K. Punch, C. H. Trinh, S. D. Dowall, R. Hewson, J. A. Hiscox,
529 J. N. Barr, and T. A. Edwards, “The crystal structure of the Hazara virus nucleocapsid
530 protein,” *BMC Struct. Biol.*, vol. 15, p. 24, 2015.
- 531 [17] S. D. Carter, R. Surtees, C. T. Walter, A. Ariza, É. Bergeron, S. T. Nichol, J. A. Hiscox,
532 T. A. Edwards, and J. N. Barr, “Structure, function, and evolution of the Crimean-Congo
533 hemorrhagic fever virus nucleocapsid protein,” *J. Virol.*, vol. 86, no. 20, pp. 10914–
534 10923, 2012.
- 535 [18] Y. Wang, S. Dutta, H. Karlberg, S. Devignot, F. Weber, Q. Hao, Y. J. Tan, A. Mirazimi,
536 and M. Kotaka, “Structure of Crimean-Congo Hemorrhagic Fever Virus Nucleoprotein:

- 537 Superhelical Homo-Oligomers and the Role of Caspase-3 Cleavage,” *J. Virol.*, vol. 86,
538 no. 22, pp. 12294–12303, 2012.
- 539 [19] W. Wang, X. Liu, X. Wang, H. Dong, C. Ma, J. Wang, B. Liu, Y. Mao, Y. Wang, T. Li,
540 C. Yang, and Y. Guo, “Structural and Functional Diversity of Nairovirus-Encoded
541 Nucleoproteins,” *J. Virol.*, vol. 89, no. 23, pp. 11740–11749, 2015.
- 542 [20] S. Wolff, S. Becker, and A. Groseth, “Cleavage of the Junin Virus Nucleoprotein Serves
543 a Decoy Function To Inhibit the Induction of Apoptosis during Infection,” *J. Virol.*, vol.
544 87, no. 1, pp. 224–233, 2013.
- 545 [21] H. Karlberg, Y. J. Tan, and A. Mirazimi, “Induction of caspase activation and cleavage
546 of the viral nucleocapsid protein in different cell types during Crimean-Congo
547 hemorrhagic fever virus infection,” *J. Biol. Chem.*, vol. 286, no. 5, pp. 3227–3234, 2011.
- 548 [22] J. Fuller, R. A. Surtees, A. B. Shaw, B. Álvarez-Rodríguez, G. S. Slack, T. A. Edwards,
549 R. Hewson, and J. N. Barr, “Hazara nairovirus elicits differential induction of apoptosis
550 and nucleocapsid protein cleavage in mammalian and tick cells,” *J. Gen. Virol.*, no. In
551 Press.
- 552 [23] C. Salata, V. Monteil, H. Karlberg, M. Celestino, S. Devignot, M. Leijon, L. Bell-Sakyi,
553 É. Bergeron, F. Weber, and A. Mirazimi, “The DEVD motif of Crimean-Congo
554 hemorrhagic fever virus nucleoprotein is essential for viral replication in tick cells,”
555 *Emerg. Microbes Infect.*, vol. 7, no. 1, p. 190, 2018.
- 556 [24] K. J. Lee, I. S. Novella, M. N. Teng, M. B. Oldstone, and J. C. de La Torre, “NP and L
557 proteins of lymphocytic choriomeningitis virus (LCMV) are sufficient for efficient
558 transcription and replication of LCMV genomic RNA analogs.,” *J. Virol.*, vol. 74, no. 8,
559 pp. 3470–3477, 2000.
- 560 [25] A. C. Lowen, C. Noonan, A. McLees, and R. M. Elliott, “Efficient bunyavirus rescue from
561 cloned cDNA,” *Virology*, vol. 330, no. 2, pp. 493–500, 2004.
- 562 [26] T. Ikegami, S. Won, C. J. Peters, and S. Makino, “Rescue of infectious rift valley fever
563 virus entirely from cDNA, analysis of virus lacking the NSs gene, and expression of a
564 foreign gene.,” *J. Virol.*, vol. 80, no. 6, pp. 2933–2940, 2006.

- 565 [27] É. Bergeron, M. Zivcec, A. K. Chakrabarti, S. T. Nichol, C. G. Albariño, and C. F.
566 Spiropoulou, “Recovery of Recombinant Crimean Congo Hemorrhagic Fever Virus
567 Reveals a Function for Non-structural Glycoproteins Cleavage by Furin,” *PLoS Pathog.*,
568 vol. 11, no. 5, 2015.
- 569 [28] C. Duclos, C. Lavoie, and J. B. Denault, “Caspases rule the intracellular trafficking
570 cartel,” *FEBS J.*, vol. 284, no. 10, pp. 1394–1420, 2017.
- 571 [29] Y. Matsumoto, K. Ohta, D. Kolakofsky, and M. Nishio, “A mini-genome study of Hazara
572 Nairovirus genomic promoters.,” *J. Virol.*, no. Epub ahead of print, Jan. 2019.
- 573 [30] R. Hewson, J. Chamberlain, V. Mioulet, G. Lloyd, B. Jamil, R. Hasan, A. Gmyl, L. Gmyl,
574 S. E. Smirnova, A. Lukashev, G. Karganova, and C. Clegg, “Crimean-Congo
575 haemorrhagic fever virus: Sequence analysis of the small RNA segments from a
576 collection of viruses world wide,” *Virus Res.*, vol. 102, no. 2, pp. 185–189, 2004.
- 577 [31] L. Bell-Sakyi, “Continuous cell lines from the tick *Hyalomma anatolicum anatolicum*,” *J.*
578 *Parasitol.*, vol. 77, no. 6, pp. 1006–1008, 1991.
- 579 [32] R. Surtees, S. D. Dowall, A. Shaw, S. Armstrong, R. Hewson, M. W. Carroll, J.
580 Mankouri, T. A. Edwards, J. A. Hiscox, and J. N. Barr, “Heat Shock Protein 70 Family
581 Members Interact with Crimean-Congo Hemorrhagic Fever Virus and Hazara Virus
582 Nucleocapsid Proteins and Perform a Functional Role in the Nairovirus Replication
583 Cycle,” *J. Virol.*, vol. 90, no. 20, pp. 9305–9316, 2016.

584

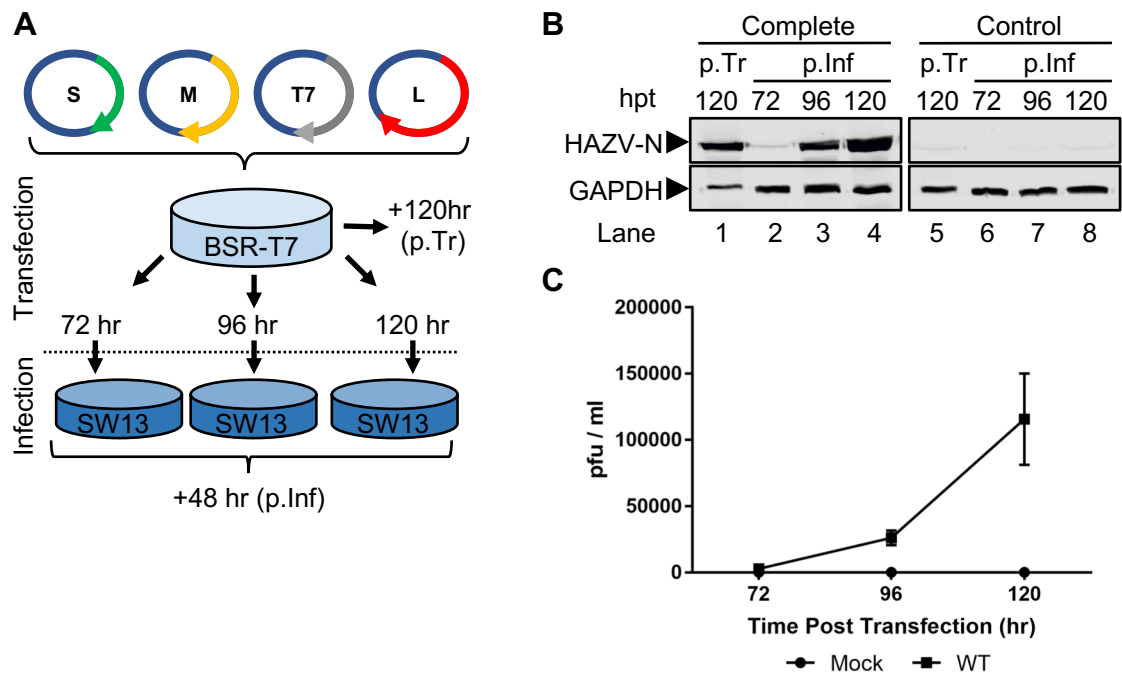
585



587

588 **Figure 1. Detection of multiple HAZV-N cleavage products.** A) Monolayers of SW13 cells
 589 were infected with HAZV at an MOI of 0.01. At the indicated hour time points post infection
 590 (hpi), total cell lysates were collected and analysed for HAZV-N expression by western blotting
 591 with HAZV-N antiserum. B) Predicted cleavage motifs of HAZV-N and associated predicted
 592 molecular weights of N' and C' fragments resulting from cleavage in Daltons. C) Schematic
 593 showing solvent-accessible location of motifs described in part B.

594



595

596 **Figure 2. Recovery of recombinant HAZV.** A) Schematic showing work-flow for recovery of

597 rHAZV. Plasmids were transfected into BSR-T7 cells for the indicated duration, prior to harvest

598 of supernatant and subsequent 48-hour infection of SW13 monolayers. B) Detection of HAZV-

599 N protein post transfection (p.Tr) of BSR-T7 cells and subsequent 48 hour post infections

600 (p.Inf). Supernatant samples collected from transfected BSR-T7 cells at 72-, 96- and 120-

601 hours post transfection (hpt) were used to infect monolayers of SW13 cells. Following a 48-

602 hour infection, lysates were collected (p.Inf, lanes 2-4) and analysed for N expression by

603 western blotting alongside lysates collected from the initial transfected BSR-T7 cells (p.Tr,

604 lane 1). Recovery of wild-type (WT) rHAZV (Complete) was carried out alongside a control

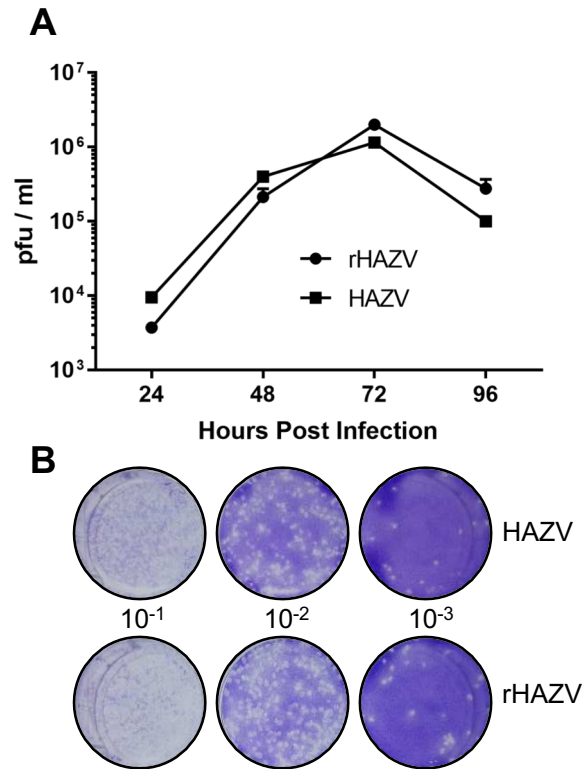
605 recovery omitting transfection of the essential pMK-RQ-L plasmid (p.Tr and p.Inf, lanes 5-8).

606 Detection of GAPDH abundance was included as a loading control. C) Titre of infectious

607 rHAZV released into supernatant at 72-, 96-, and 120-hour time points p.Tr was assessed via

608 plaque assay, error bars represent average of two repeats.

609



610

611 **Figure 3. Growth kinetics of rHAZV versus parental isolate, A)** Titre of infectious rHAZV

612 (circle) and its parental strain of HAZV (square) harvested at 24-hour intervals for 4 days

613 following infection of SW13 cells at an MOI of 0.001. B) Representative plaque assays used

614 to determine titre of infectious HAZV and rHAZV in (A) showing plaque morphology to be

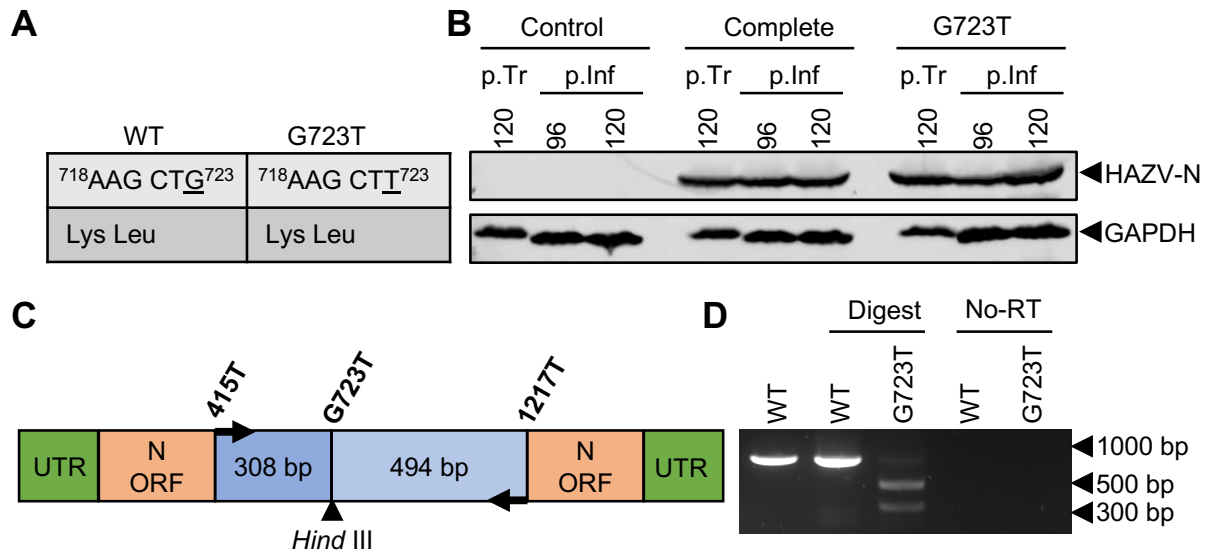
615 similar in both instances. Serial dilutions were generated from virus harvested 24 hours post

616 infection and used to infect SW13 monolayers for 1 hour prior to addition of a methyl cellulose

617 overlay. Cells were then fixed and stained 6 days post infection and viral plaques were

618 counted.

619



620

621

622 **Figure 4. Confirmation of cDNA origin via recovery of mutant rHAZV.** A) Table outlining

623 the change (underlined) to both cDNA sequence of the HAZV-N ORF and the resulting amino

624 acid sequence. B) Detection of HAZV-N by western blotting following transfection (p.Tr) of

625 BSR-T7 cells and subsequent 48 hour infections (p.Inf). Supernatant samples collected from

626 transfected BSR-T7 cells at 96 hours p.Tr were used to infect monolayers of SW13 cells.

627 Following a 48-hour infection, lysates were collected and analysed by western blotting for N

628 expression. Recovery of rHAZV containing a *Hind* III restriction site (rHAZV-G723T) was

629 carried out alongside a complete and control recovery of rHAZV. Detection of GAPDH

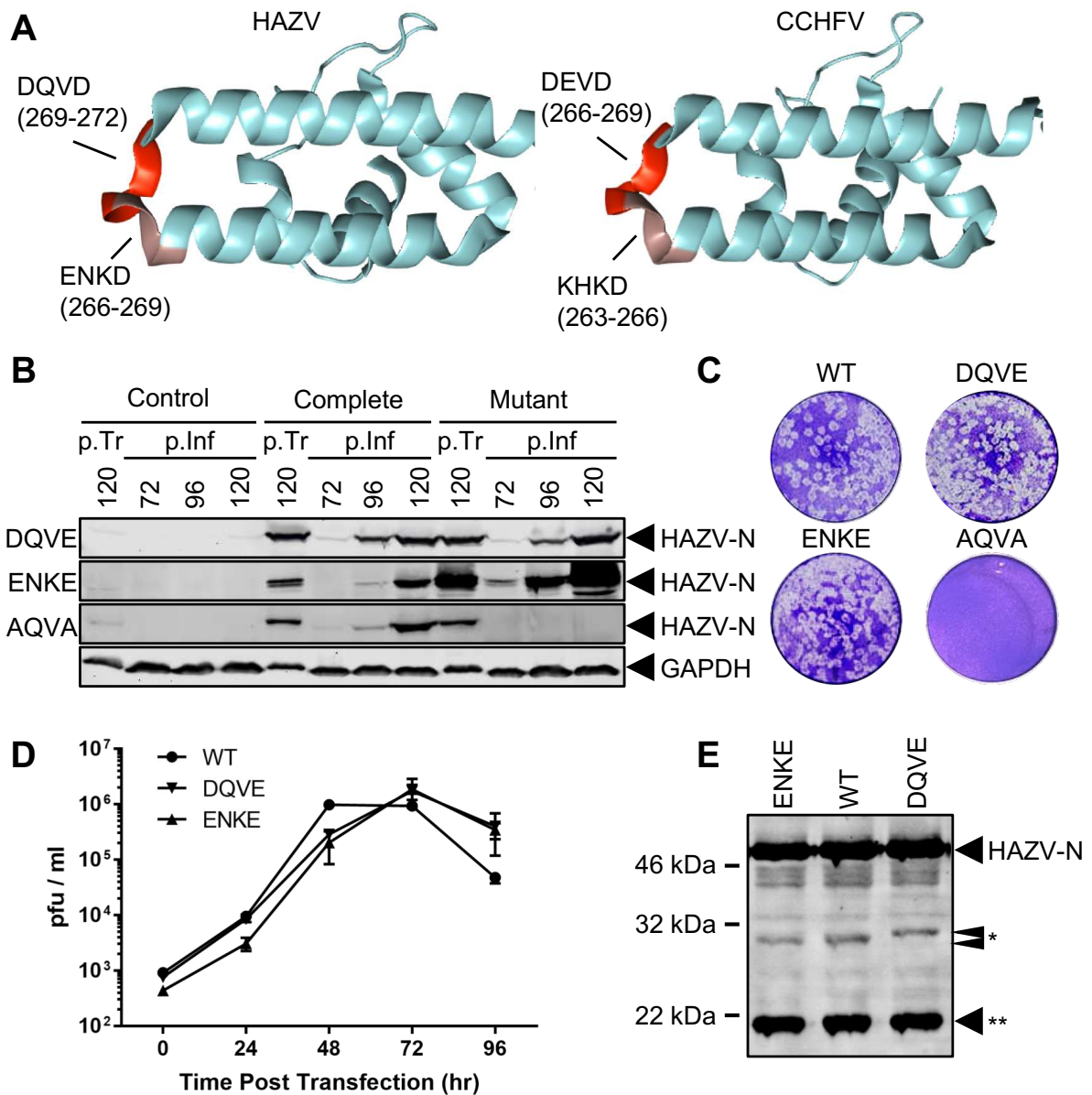
630 abundance was included as a loading control. C) Schematic showing the location of the

631 inserted *Hind* III restriction site into the S-segment ORF cDNA. D) Restriction digest of dsDNA

632 fragment following RNA extraction of rHAZV and rHAZV-G723T containing supernatants, first

633 strand synthesis and PCR amplification of viral genetic material.

634



635

636

637 **Figure 5. Recovery of mutant rHAZV targeting multiple caspase motifs.** A) Schematic

638 showing location of caspase cleavage motifs on the apex of the arm domains for HAZV and

639 CCHFV, with amino acid positions indicated numerically. B) Western blot detection of HAZV-

640 N protein for rHAZV-DQVE, ENKE and AQVA mutants following transfection (p.Tr) of BSR-T7

641 cells and subsequent 48 hour infections (p.Inf) of SW13 cells using supernatant harvested 72-

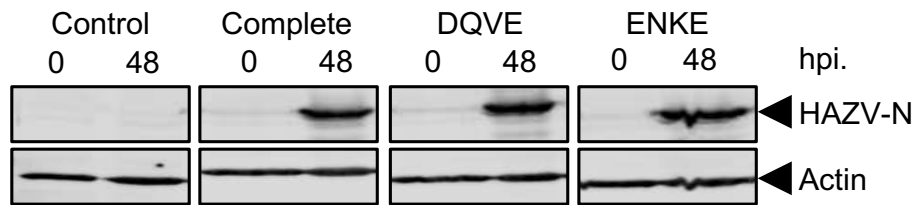
642 , 96- and 120-hours p.Tr. Recovery of all mutants was carried out alongside independent

643 complete and control recoveries of WT rHAZV. Detection of GAPDH abundance was included

644 as a loading control. C) Representative plaque assays from supernatant taken 120 hours p.Tr

645 displaying plaque morphology for recovered viruses. D) Titre of infectious WT rHAZV (circle)
646 versus DQVE (triangle↓) and ENKE (triangle↑) at 24-hour intervals following infection of SW13
647 cells at an MOI of 0.001. E) Detection of HAZV-N and associated cleavage products at 30 and
648 32 kDa (*) and 20 kDa (**) following a 48-hour infection at an MOI of 0.01.

649



650

651 **Figure 6.** The ability of rHAZV, rHAZV-DQVE and rHAZV ENKE to replicate in the tick cell line
652 HAE/CTVM9 was examined via western blot detection of HAZV-N in lysates taken 48 hours
653 post infection (hpi) at an MOI of 0.01. Actin was included as a loading control.

654